Measuring Exposure to Extreme Heat in Public Transit Systems

Luyu Liu [1, 2, *], Xiaojiang Li [3], Xiang Yan [2], Rafael H.M. Pereira [4]

[1] Department of Geosciences, Auburn University, Alabama, USA

[2] Department of Civil and Coastal Engineering, University of Florida, Florida, USA

[3] Weitzman School of Design, University of Pennsylvania, Pennsylvania, USA

[4] Institute for Applied Economic Research, Brasília, Brazil

Abstract:

Public transit users are among the most vulnerable to extreme heat due to urban heat island effect and longer outdoor exposure. However, few studies have investigated transit riders' heat exposure and considered exposure time and travel behavior when calculating heat exposure. This paper introduces a holistic measurement system – *Transit Heat Exposure Index* (THEI) – to gauge high-fidelity heat exposure for transit riders and apply the method to Miami, one of the hottest US cities. By using high-resolution meteorological and built environment data, we calculate 1m-by-1m feels-like temperature for Miami-Dade Transit with microclimate simulation techniques. Then, we calculate the detailed travel time between all census block groups in Miami with realistic transit routing technique. We then adopt a *total time-degree* approach to calculate heat exposure and aggregate THEI at

* Corresponding author, email: liuluyu0378@gmail.com, ORCID: 0000-0002-6684-5570

different levels. Our results show that despite higher local feels-like temperature, downtown Miami has lower heat exposure due to better transit access. Source analysis also shows that walking is the primary source of heat compared to waiting, and a small portion of streets and bus stops contribute most heat exposure. This method provides first-hand evidence for future heat planning, enabling more effective strategies to mitigate extreme heat's impact on transit riders.

Keywords: Heat Exposure; Public Transit; Urban Heat Island Effect; Microclimate Simulation; Thermal Comfort; Transit Heat Exposure Index.

Measuring Exposure to Extreme Heat in Public Transit Systems

Abstract:

Public transit users are among the most vulnerable to extreme heat due to urban heat island effect and longer outdoor exposure. However, few studies have investigated transit riders' heat exposure and considered exposure time and travel behavior when calculating heat exposure. This paper introduces a holistic measurement system – *Transit Heat Exposure Index* (THEI) – to gauge high-fidelity heat exposure for transit riders and apply the method to Miami, one of the hottest US cities. By using high-resolution meteorological and built environment data, we calculate 1m-by-1m feels-like temperature for Miami-Dade Transit with microclimate simulation techniques. Then, we calculate the detailed travel time between all census block groups in Miami with realistic transit routing technique. We then adopt a *total time-degree* approach to calculate heat exposure and aggregate THEI at different levels. Our results show that despite higher local feels-like temperature, downtown Miami has lower heat exposure due to better transit access. Source analysis also shows that walking is the primary source of heat compared to waiting, and a small portion of streets and bus stops contribute most heat exposure. This method provides first-hand evidence for future heat planning, enabling more effective strategies to mitigate extreme heat's impact on transit riders.

Keywords: Heat Exposure; Public Transit; Urban heat island effect; microclimate simulation; thermal comfort; Transit Heat Exposure Index.

Highlights:

- Transit Heat Exposure Index offers a new mobility-based method to measure heat exposure for transit users.
- Despite higher local temperatures, downtown Miami has lower overall heat exposure due to better transit service.
- Walking, not waiting, is the primary source of transit heat exposure in Miami.
- A small percentage of street links and bus stops cause most heat exposure.
- THEI provides firsthand evidence for effective strategies to reduce heat exposure for transit riders.

1. Introduction

Extreme heat events present significant risks to public health, infrastructure security, and the environment. Extreme heat can cause heat exhaustion and heat stroke, which exacerbates preexisting conditions and increase mortality (Dong et al., 2020; Ebi et al., 2021; McMichael, 2020). Heat is also a critical social equity issue: it disproportionately affects vulnerable and marginalized population due to disparities in access to cooling, housing, mobility, and workplace conditions (Gu et al., 2024; Turek-Hankins et al., 2020). As extreme heat events are projected to become more frequent and severe due to climate change, exposure and heat-related incidents will become increasingly important issues in urban environments (Klein & Anderegg, 2021).

Transportation is a major source of heat exposure, especially for public transit riders (Fraser & Chester, 2017). Compared with other motorized modes of transportation, public transit riders experience more extreme heat exposure due to three factors. First, public transit users spend more time outside the vehicle Because public transit users often need to walk for some distances to access transit stops and during transfers (Bowman & Turnquist, 1981; Liu et al., 2022). Second, public transit users may also experience long wait times due to low service frequency and low reliability. Third, urban areas with intensive public transit service and more transit-dependent populations generally have higher average temperatures due to urban heat island effect (Hsu et al., 2021; Yin et al., 2023). The lack of heat-aware infrastructure such as tree canopy and shades at transit stations and along pedestrian paths can exacerbate the heat exposure experienced by transit riders (Cheung, 2018; X. Li, 2021). As socially disadvantaged and marginalized groups tend to rely on public transit services and lack reliable transportation alternatives, transit heat exposure is a major equity issue to be addressed (Dzyuban et al., 2021; Karner, 2018).

Despite a growing number of studies on extreme heat and mobility patterns, most of these studies overlook heat exposure in public transit (Gu et al., 2024; Huang et al., 2024; R. Li et al., 2023). The existing studies that focus on transit heat exposure have various limitations. First, most prior studies do not consider travel behavior (e.g., travel time and route choice) as a factor in the calculation of heat exposure (Kuras et al., 2017; Nazarian & Lee, 2021), even though exposure time can be as important as the local temperature. Second, despite abundant studies on the community-level thermal comfort and urban heat island effect, there is a lack of high-resolution, individual-level heat exposure (Kuras et al., 2015). Finally, although the general patterns of heat exposure have been extensively discussed, the source of exposure is not yet fully understood. Public transit riders' heat exposure come from three major components: *walking time*, which happens during the first and last mile of the transit trip on street links, *waiting time*, which happens before boarding at bus stops, and *in-vehicle time*, which happens inside the vehicle. This study ignores *in-vehicle time* because most buses in the U.S. have air-conditioning onboard. To our best knowledge, no prior studies investigated and compared the respective contributions of walking and waiting to transit heat exposure. Meanwhile, the methods used in previous studies are not able to provide spatially detailed information on where and when transit users would suffer heat exposure the most.

In light of the research gaps discussed above, this paper introduces a novel methodology to measure high-resolution network-based heat exposure for public transit riders. The proposed method combines microclimate simulation and realistic transit network routing methods, which allows one estimate how exposure during walking at street links and waiting at bus stops contribute the overall heat exposure of public transit riders. We demonstrate the proposed method with a case study of Miami, Florida. To do this, we use high-resolution meteorological data, tree canopy, and building LiDAR data to calculate a 1m-by-1m feels-like temperature map, as well as General Transit Feed Specification (GTFS) data and a state-of-the-art transit routing to generate high-fidelity travel itinerary between all census block groups. Combining these two data products with the Longitudinal Employer-Household Dynamics (LODES) empirical commuter flows, we create a new transit-based heat exposure measure – Transit Heat Exposure Index (THEI), which can be examined to indicate the total or the average experience of heat on public transit trips. Our method also allows one to examine the total or average exposure to heat on public transit trips experienced by passengers departing from specific origins and by passengers travelling to specific destinations. The proposed method provides detailed results so that researchers and policymakers can more effectively understand heat exposure nuances and devise strategies to mitigate its public and urban impacts.

The paper is structured as follows. We first review the prior literature about the measurement of extreme heat and public transit in section 2. We then introduce our data and method in section 3. We then present our results and discussion in section 4. We finally conclude the paper with some high-level insights to provide useful guidance for future research and practical planning.

2. Background

This section reviews a brief review of the literature on the domain of extreme heat exposure and public transit. It is organized into four subsections. We first discuss the evolution of extreme heat exposure. Next, we review the research on the implications of the built environment for heat exposure in cities. We finally review the literature about heat exposure and public transit and summarize the research gaps in current literature.

2.1. Measuring Extreme Heat Exposure in Urban Areas

The history of measuring extreme heat exposure has evolved significantly in recent decades, reflecting advancements in technology and a growing understanding of heat's impact on both the environment and human health (Deschenes, 2014; Wong et al., 2013). In the early stages, basic thermometry was the primary method for measuring ambient temperatures. However, these methods were limited in scope, focusing solely on ambient temperature without considering other environmental factors or human physiological responses to heat. Technological progress, such satellite imaging, enabled large-scale monitoring of surface temperatures and the identification of heatwaves, significantly enhancing our ability to track and analyze global heat exposure trends (Shandas et al., 2019). Additionally, the field of biometeorology introduced human-centric measures, integrating human physiological responses to heat into the assessment of heat exposure (Kuras et al., 2017). This led to the development of thermal comfort models like the Predicted Mean Vote (PMV) (Yau & Chew, 2014) and Standard Effective Temperature (SET) (Iseki & Tingstrom, 2014). More recent progresses include Mean Radiant Temperature (MRT) (Thorsson et al., 2014) and Universal Thermal Climate Index (UTCI) (Błażejczyk et al., 2013), which marked a shift towards a more nuanced understanding of heat exposure, considering not just environmental parameters but also their direct impact on human health and well-being.

As there are extensive discussions on extreme heat exposure and the impacts of urban heat island and climate change, most research focus on the post-event outcomes such as heat mortality and morbidity (Benmarhnia et al., 2015; Nazarian & Lee, 2021), and there remains a significant knowledge gap about the immediate, real-time experiences of thermal discomfort and the physical strain individuals experience, especially public transit.

2.2. Heat Exposure and Built Environment

Built environment has major impacts on the exposure of extreme heat, especially for urban dwellers (Nazarian & Lee, 2021). One of the central themes in this body of research is the urban heat island (UHI) effect, which refers to the phenomenon of urban areas experiencing higher temperatures than their rural surroundings (Hsu et al., 2021; Yin et al., 2023).

UHI is driven by three main factors: land cover and albedo, urban tree canopy, and buildings. Urban areas often consist of impervious surfaces such as concrete and asphalt, which have low albedo, meaning they absorb and retain heat (Obiakor et al., 2012). This contributes to increased temperatures within cities. Meanwhile, tree canopy and buildings can provide shades that reduce heat, while trees can have more cooling effects via evaporation (Cheung, 2018). Previous research has shown that tress can lead to average daytime cooling impacts of 0.6 °C for air temperature and 2.5°C for feels-like temperature, surpassing those of concrete shelters, which recorded 0.2 °C for air temperature and 2.0 °C for feels-like temperature, respectively (Cheung, 2018).

2.3. Heat Exposure and Public Transit

Very few papers have investigated the heat exposure of public transit riders. Karner et al. (2015) was among the first to discuss the heat exposure of public transit as well as other non-motorized travel modes, including walking and biking. By using simulated travel and 1km resolution air temperature data, the authors revealed that disadvantaged groups are disproportionately affected by extreme heat. Fraser et al. (2017) estimated exposure from walking and waiting by using shortest distance from nearest bus stop and bus schedule. The paper found that users from low-density and low-connectivity areas would have higher expected exposure due to longer walking distances and waiting times. Meanwhile, Dzyuban et al. (2021) surveyed public transit riders about their perceptions of heat and behavior changes to cope with heat in Phoenix, AZ.

The heat levels experienced by public transit users is also sensitive to the built environment such as tree canopies and building shades. Nevertheless, unique to public transit systems, bus shelters can also impact the heat experience of transit users, but there are mixed conclusions from prior studies. For example, Miao et al. (2019) studied the links between extreme weather, including very high and very low temperature, and public transit ridership and found significant moderating effect of bus shelters. However, Lanza & Durand (2021) examined the impacts of bus shelter availability to the public transit ridership in Austin, TX and found shelters did not moderate the effect of high temperature on ridership, but tree canopies did have moderating effect. Finally, Sami & Keith (2023) conducted a survey on the outdoor thermal comfort perceptions of passengers of the Sun

Link streetcar in Tucson, Arizona, and concluded that perceptions of heat varied substantially according to transit stop design.

2.4. Research Gaps

There are some important gaps in the literature on public transit users' heat exposure. First, most of the prior studies do not consider exposure time as a factor. Nonetheless, in real-world scenarios, a person's experience and risk of heat stress are highly susceptible to prolonged exposure to high-temperature environments. In other words, most prior studies assume that all transit passengers are equally exposed to heat for the same amount of time, regardless of different spatiotemporal contexts of travel heavier patterns.

Prior studies also lack high-resolution heat exposure measurements that consider place-to-place transit trip experience and built environment impacts. Kuras et al. (2017) pointed out that prior studies use an implicit assumption that population's heat exposure can be estimated from data based on outdoor conditions. The paper also pointed out that most research assumes some level of homogeneity, even though heat exposure is a highly personalized and heterogeneous process. Meanwhile, Nazarian & Lee (2021) reviewed 122 publications on urban heat exposure and concluded that the spatial and temporal variability of heat exposure in cities is not fully incorporated in urban heat research. The paper also concluded that although large-scale individual heat exposure assessments are impractical, it is feasible to broadly categorize heat conditions across the built environment with fine-scale assessment.

3. Methods

Here we introduce our proposed method. We first present the site of our case study and the data we used. We then describe the two major methodological steps, which involve calculating high-resolution thermal comfort data and detailed itineraries. Next, we explain how the results of these two steps are combined to calculate our proposed new metric – *Transit Heat Exposure Index (THEI)* – to measure the extent and spatiotemporal patterns of heat exposure of public transit riders. Finally, we explain how this metric can be analyzed to decompose total heat exposure into network-based exposure during walking and waiting times.

3.1. Data

In this study, we utilize diverse datasets from various sources to measure thermal comfort and travel behavior of public transit riders.

Transit data. We use the General Transit Feed Specification (GTFS) schedule data, which is the *de facto* data standard for public transit schedule timetable (Google Developers, 2020). The GTFS data for Miami-Dade County Transit are captured near August 1st, 2023 and collected from the Transitfeeds.com (OpenMobilityData, 2023). We use the OpenStreetMap network data in September 2023 as the data source of sidewalk network.

Meteorological data. We collect the meteorological data, including air temperature, global horizontal radiation, direct radiation, diffuse radiation, and relative humidity data, from the NREL data portal (NREL, 2024). All data are collected at the latest available timepoint, i.e., August 2020.

Built environment data. The building footprint map was collected from Microsoft building footprint database (Microsoft, 2018/2024). The most recent high-resolution LiDAR cloud point datasets from United States Geological Survey (U.S Geological Survey, 2023) were used to generate the digital surface model (DSM) with a spatial resolution of 1m. The multispectral NAIP imageries with a spatial resolution around 1m were used to generate the tree canopy cover maps using the thresholding method on the normalized difference vegetation index (NDVI) (National Agriculture Imagery Program, 2023). The tree canopy cover maps were then refined based on the generated DSM by removing those pixels lower than 2 m, since the shade of trees lower than 2m is negligible. The building footprint map and the generated tree canopy map were then overlayed on the DSMs to generate the building height model and tree canopy height model for the study area.

Our case study focuses on the city of Miami, Florida, USA. Florida is one of the most vulnerable areas to heat exposure and heat-related mortality in the United States (Curriero et al., 2002; Keellings & Waylen, 2014), and Miami is among the hottest city in the US with an average annual temperature of 26°C from 2009 to 2021 (World Weather Online, 2024); The hottest month ever recorded was July 2023, when the temperature was higher than 37°C for 46 consecutive days in Miami (Crowley, 2023). Heat-related mortality in Miami was also reported to be much higher than northern cities in the US (Curriero et al., 2002), with the duration and frequency of the extreme heat events projected to be much higher due to climate change (McAllister et al., 2022). Furthermore, Florida is the third most populous state in the US with over 20% of its population older than 65 years old, who are more susceptible to heat exposure and heat-related illnesses (US Census Bureau, 2020).

3.2. Feels-like Temperature Calculation

The mean radiant temperature (T_{mrt}) is the net shortwave and longwave radiation to which human body exposed from the surrounding environment and the T_{mrt} is the most significant meteorological input parameter for the human energy balance especially during clear and calm summer days (Mayer & Höppe, 1987). Based on the Stefan-Boltzmann law, T_{mrt} can be calculated as,

$$T_{mrt} = \sqrt[4]{R/_{\varepsilon_p \sigma}} - 273.15 \quad (1)$$

where ε_p is the emissivity of the human body (standard value 0.97), σ is the Stefan-Boltzmann constant, and R denotes total radiation exposure as the sum of short and long wave radiation from above, below, and the four cardinal directions, and the R can be calculated as,

$$R = \xi_k \sum_1^6 K_i F_i + \varepsilon_p \sum_1^6 L_i F_i \quad (2)$$

where K_i is the shortwave radiation component from 6 directions (north, south, west, east, top and bottom), L_i is the longwave radiation, F_i is the angular factor between a person and the surrounding environment, ξ_k is the absorption coefficient for shortwave radiation (standard value 0.7). This study adopted the previously developed GPU-accelerated SOlar and LongWave Environmental Irradiance Geometry model (SOLWEIG) model (X. Li & Wang, 2021) to calculate the T_{mrt} based on the input and the meteorological data (Figure 1).

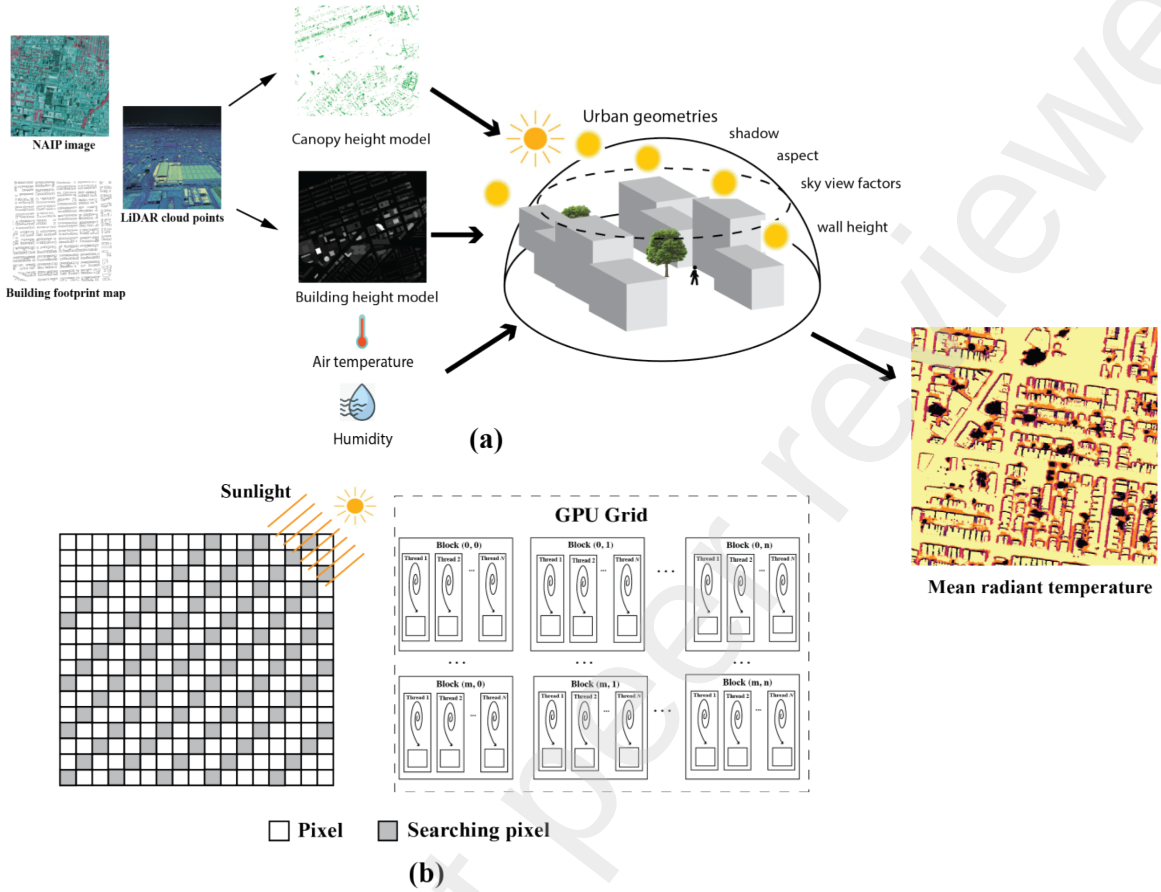

Figure 1: The calculation of the T_{mrt} using the SOLWEIG model based on tree canopy height model, building height model, and meteorological data using the GPU-accelerated algorithm, (a) the SOLWEIG model for computing the mean radiant temperature, (b) the GPU structure.

3.3. Realistic Transit Routing

To accurately represent the transit experience of a public transit rider, we employ realistic transit routing techniques to calculate door-to-door detailed itineraries of transit trips in the form of Origin-destination matrix. The first step is to determine the origins and the destinations (OD) of the transit trips. We choose the centroids of census block groups as the OD for three reasons: first, census block groups are the smallest geographic units with the most updated and comprehensive sociodemographic information, which can provide a more refined patterns of the heat exposure in space. Second, the LODES data are based on census blocks, which can be combined to each census block group and serve as the weight when aggregating the heat exposure measure. The final reason is performance consideration. Due to the nature of OD matrix, the computational load will increase quadratically with more ODs. Census block groups are a perfect balance of finer-grained measurement and manageable computational cost.

The second step is to calculate the shortest path between each OD pair. We use an open-source solution – *r5r* – an R package that calculates rapid realistic routing for multimodal transportation networks (Pereira et al., 2021). The package uses a Java-based routing engine, i.e., R5, and a R wrapper to achieve fully paralleled routing calculation with very high performance (Higgins et al., 2022). The package ingests GTFS schedule data and OpenStreetMap network data to construct a routable transit network.

We utilized r5r's *detailed itinerary* function, which outputs the detailed trip information between origin-destination pairs, including first/last-mile walking time, waiting time, in-vehicle time, and geometries for each trip. We set the maximum walk time as 30 minutes, the maximum trip duration as 60 minutes, walk speed as 1 m/s, and maximum rides as 3. Since the departure time chosen for trips significantly influences trip routing outcomes due to the uncertainty of when the next bus will arrive at the transit stop (Stewart & Byrd, 2023), we calculated for each OD pair several trip itineraries departing every minute over a time window of 7 minutes starting from noon considered the trip itinerary with the median travel time. We also combine all the itinerary from August 1st to August 7th, 2023 and calculate the average travel time.

The current version of the package does not output disaggregated information on the links and stops in the network, which requires users to conduct spatial join and is very time consuming and inefficient. To address this limitation, we modify the Java code to output the corresponding link IDs in the Open Street Map network and boarding and alighting bus stop information. We then import the large amount of CSV files generated by the package and synthesize the data into organized records in a single collection in a MongoDB database.

3.4. Exposure Measurement

With the feels-like temperature and the exposure time at each corresponding trip leg in each trip from and to the centroids of census block group, we introduce the Transit Heat Exposure Index (THEI), a new measure that considers both temperature and temporal factors. We adopt a *total degree-second* approach, i.e., the sum product of feels-like temperature and exposure time, to construct the measurement similar to Karner et al. (2015). Compared with air or ground temperature, MRT can better capture personal thermal comfort experience; MRT is also more suitable in the sense of thermodynamics as MRT is an additive measure of the net exchange of radiant energy between the human body and the surrounding environment. We define the heat exposure from census block group i to j as:

$$h_{ij} = h_{ij}^t + h_{ij}^w + h_{ij}^v = \sum_k t_{ijk}^t \cdot T_{ijk}^t + \sum_l t_{ijl}^w \cdot T_{ijl}^w \tag{3}$$

The total heat exposure can be decomposed into three sections based on the environment the users are experiencing in a typical transit trip: h_{ij}^t, i.e., walking along a road link, h_{ij}^w, i.e., waiting at a bus stop, and h_{ij}^v, i.e., riding in a vehicle.

- **Walking.** t_{ijk}^t is the walking travel time along road segment k when travelling from origin i to destination j, including first-mile, last-mile, and transfer. ΔT_{ijk}^t is the cumulative radiant during the link, which is a function of air temperature, humidity, solar radiation factor, tree canopy, and building cover in the road segment k.
- **Waiting.** Similarly, t_{ijl}^w is the waiting time at stop l when travelling from origin i to destination j, and T_{ijl}^w is the feels-like temperature at stop l.
- **In-vehicle.** In this study, we assume that users do not suffer from heat exposure in the vehicles, since all buses in Miami have air conditioning. However, it is also important to note that this assumption only hold for the context of United States. For many cities in the Global South, heat exposure when riding is an equally important issue and might be aggravated due to passenger crowding (Arbex & Cunha, 2020).

To calculate the feels-like temperature at each road link T_{ijk}^t and at each bus stop T_{ijl}^w, we conduct the overlay operation on the generated MRT raster against the road network and the bus stops, respectively using the method *ZonalStatisticsAsTable* in ArcGIS Pro. For exposure on the road links, we calculate the mean of the MRT raster that intersects with the road's geometry. We then calculate the total exposure on the road link by the mean MRT multiplied by walking time in seconds, i.e., the road links' length divided by walking speed of 1 m/s, which the default average walking time used in the routing engine. For the exposure at the bus stops, we also use the ZonalStatisticsAsTable function to calculate the mean exposure at each stop point, and we calculate the exposure by multiplying the mean exposure by the waiting time.

3.5. Analysis

With the heat exposure measured for each individual OD pair, we perform aggregations at various analytical levels to better understand the spatiotemporal patterns.

Total Transit Heat Exposure Index (Total THEI). We introduce *total THEI to* capture the sum of the potential heat exposure that would have been experienced by transit riders travelling between all origin-destination pairs weighted by the number of trips between each OD pair. As such, total THEI consists of two components: one is the *potential* exposure of each trip, and the other is the number of passengers taking those trips. When taking the trip origins as a reference, total THEI is defined as

$$H_i^o = \sum_j w_{ij} \cdot h_{ij} \qquad (4)$$

Where H_i^o is the origin-based total exposure for the origin i. h_{ij} is the heat exposure for the OD link. Note that we aggregate the OD links to their origin here, which measures the total exposure experienced by riders departing from the census block group i when accessing all other destinations. w_{ij} is a weight to aggregate the exposure of different OD pairs, which can be based on actual ridership, potential demand, or local and destination demographics.

Here we use the most recent commuter flows in 2021 from Longitudinal Employer-Household Dynamics (LODES) data as proxies for potential trips across OD pairs.

We also aggregate the OD links to their destination and produce a destination-based heat exposure, which measures the exposure experienced by all riders that travel to the census block group j. It is defined as

$$H_j^D = \sum_i w_{ij} \cdot h_{ij} \tag{5}$$

Where H_j^D is the destination-based total exposure to the destination j.

Mean Transit Heat Exposure Index (Mean THEI). Total THEI or total exposure is a function of three factors: 1) the feels-like temperature at the waiting stops and the street links, 2) the average travel time, and 3) the number of trips originated to/from a given locations. In other words, with more ridership or demand between the OD pair, the total exposure will increase. Therefore, to gauge transit-based heat exposure with a temperature-esque measure, we introduce the *mean THEI.* It is a measure of average level of heat exposure experienced by transit riders during their transit trip experience. It is defined as:

$$e = \frac{H}{t} = \frac{\sum w_{ij} \cdot h_{ij}}{\sum t_{ij}} \tag{6}$$

Where: H is the total THEI, which could be aggregated to the origins, destinations, or networks. t is the total travel time, which is calculated as the sum of all trips, including the walking, waiting, and in-vehicle time. Note that the unit of e is Celsius, the same as temperature. The measure represents the heat that public transit users experienced in a single unit amount of time, which is independent of the number of trips made.

Similar to the total exposure, mean THEI can also be calculated for the entire transit systems or using the origin-base and destination-based versions of the measure.

Heat exposure composition from walking and waiting. It is largely unknown from prior studies that if walking or waiting is responsible for most of the heat and the specific composition of the heat generated from the two processes. A major advantage of the method introduced in this paper is the ability to produce high-resolution heat exposure measure in a very detailed level for each segment of a trip, which allows one to decompose the total heat exposure due to exposure during walking and waiting times. The share of heat from walking time can be calculated as:

$$r = \frac{H^w}{H^t + H^w} \tag{7}$$

Where r is the share of heat exposure from walking, H^t is the total THEI from waiting, and H^w is the total THEI from walking.

Network-based heat exposure. The THEI metric proposed here can also be understood as a network-based heat exposure. It measures the contribution of each road link and bus stop to total heat exposure by considering the time spend by the total number of users that traverse each road or wait at each stop. The contribution of each road link and stop to total heat exposure is defined as

$$H_k^T = \sum_{ij} w_{ij} \cdot h_{ijk} \tag{8}$$

Where: H_k^T is the exposure contribution of a road or a stop T, and h_{ijk} is the heat exposure experienced at the road/stop k by a user traveling from census block i to census block j. In practice, we calculate three measures: 1) total exposure of each road when walking, which measures the heat contribution of the road to all users' heat exposure, 2) total exposure for each bus stop when waiting, which measures the heat contribution of the bus stop to all users' heat exposure, and 3) the sum of the two exposures aggregated their corresponding census block group. We use the spatial join function with largest overlap operation in the ArcGIS Pro to calculate the third measure, which means if a street link cross two census block groups, we will be aggregating its heat to the census block group with which it has the largest overlap.

4. Results

4.1. Spatiotemporal Pattern of THEI

Figure 2 visualizes the total exposure in each census block group for Miami in quantile classification. We find that, in general, the accumulated heat exposure to heat of transit passengers travelling to and from neighborhoods in the suburban areas is rather low. This occurs largely because there are very few transit trips to and from these neighborhoods due to low transit connectivity. However, it is also noteworthy that the core of the downtown also presents lower total exposure which generally have higher local feels-like temperature and higher amounts of public transit trips and higher accessibility.

This counter-intuitive results arise because THEI considers human mobility behavior when calculating heat. Total THEI is dependent on three components: potential exposure time, temperature values, and number of trips. While the downtown is generally a heat island with higher local temperature, it usually has more frequent transit services and higher density, which makes the residents there wait less and walk less (discussed more later). Meanwhile, the weight, i.e., commute flow, is also higher in downtown. Therefore, number of trips, feels-like temperature, and exposure time can have heterogenous effect on the outcomes: higher feels-like temperature, higher number of trips, and higher exposure time can all contribute to a higher total exposure.

Meanwhile, Figure 2 shows the resemblance between the origin-based and destination-based measures. It can be because unconnected areas generally have both lower access to and from other places, and most public transit routes are symmetrical, which means the trips back and forth generally have similar travel time and geometries.

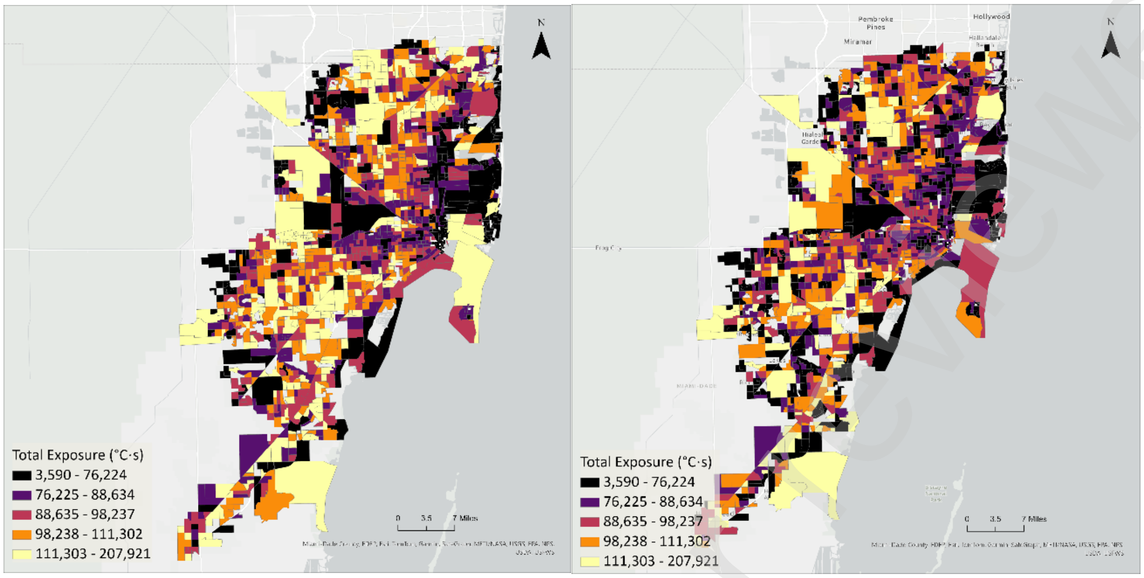

Figure 2: Total THEI of every census block group in Miami. Left: aggregated by origin; right: aggregated by destination. Maps are generated per the origin-based layer's quantile classification.

Mean THEI. In contrast to total THEI, the mean THEI is not affected by the total number of transit riders. It is only shaped by feels-like temperature values and exposure time. To investigate the patterns of the average heat exposure, we further visualize the heat exposure intensity in Figure 3. A primary observation is that transit heat exposure intensity in Miami downtown core is significantly lower than their urban outskirts and suburbs. This means that the average experienced heat in a unit amount of time when a resident is accessing other opportunities via public transit is lower in the downtown core. The downtown areas generally have higher level of transit infrastructure and sidewalk infrastructure, which reduces walking, waiting, and transfer time (Liu & Miller, 2020; Wang & Cao, 2017). For example, the exposure from walking in downtown tends to be much lower since downtowns have much higher density, more high-level buildings and tree canopies , and more extensive sidewalk network (X. Li, 2021; Liu et al., 2023). Moreover, the exposure during waiting would also tend to be lower due to higher frequency for transit routes in downtown area.

Meanwhile, like the total exposure, the origin-base and destination-based measures are highly similar for the same reasons stated above. There could be factors that contribute to the minor differences, such as differences in transit geometries and travel time and asymmetrical commute flow from and to the location.

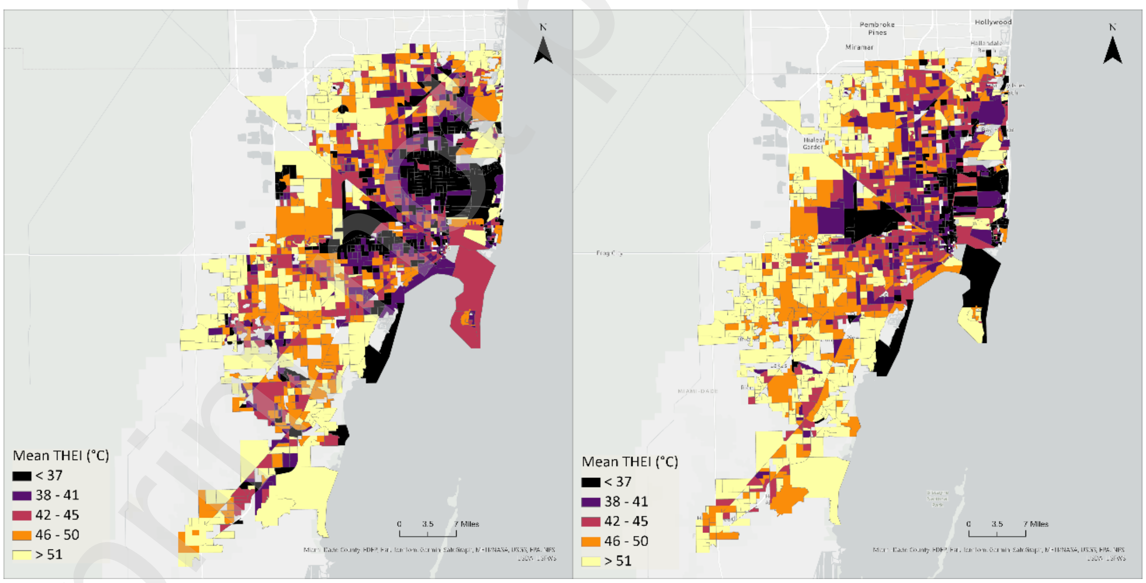

Figure 3: Mean THEI of every census block group in Miami. Left: aggregated by origin; right: aggregated by destination. Maps are generated per the origin-based layer's quantile classification.

4.2. Source of Heat Exposure

Figure 4 visualizes the heat exposure from walking and waiting, respectively. Note that we aggregate the heat to their origin, meaning that the measures represent the heat experience of local residents when accessing other opportunities. First, between walking and waiting, walking accounts for most of the heat exposure in Miami. Figure 5 also visualizes the share of exposure from walking out of the total heat exposure. This confirms that walking is the main source of heat exposure in Miami with a global average of 86%, meaning that 86% of heat exposure is from walking during first mile, last mile, and transfers, and only 14% of heat exposure is from waiting at bus stops. In practical sense, this provides a firsthand evidence that future interventions should prioritize improving the walking experience of public transit passengers, despite being a functional but not an intrinsic part of the public transit system and outside transit authorities' responsibility. Second, Figure 4 also visualizes the histogram of the two maps, and the two values have very different patterns. Interestingly, heat exposure from walking follows a normal distribution, while heat exposure from waiting follows a log-normal distribution.

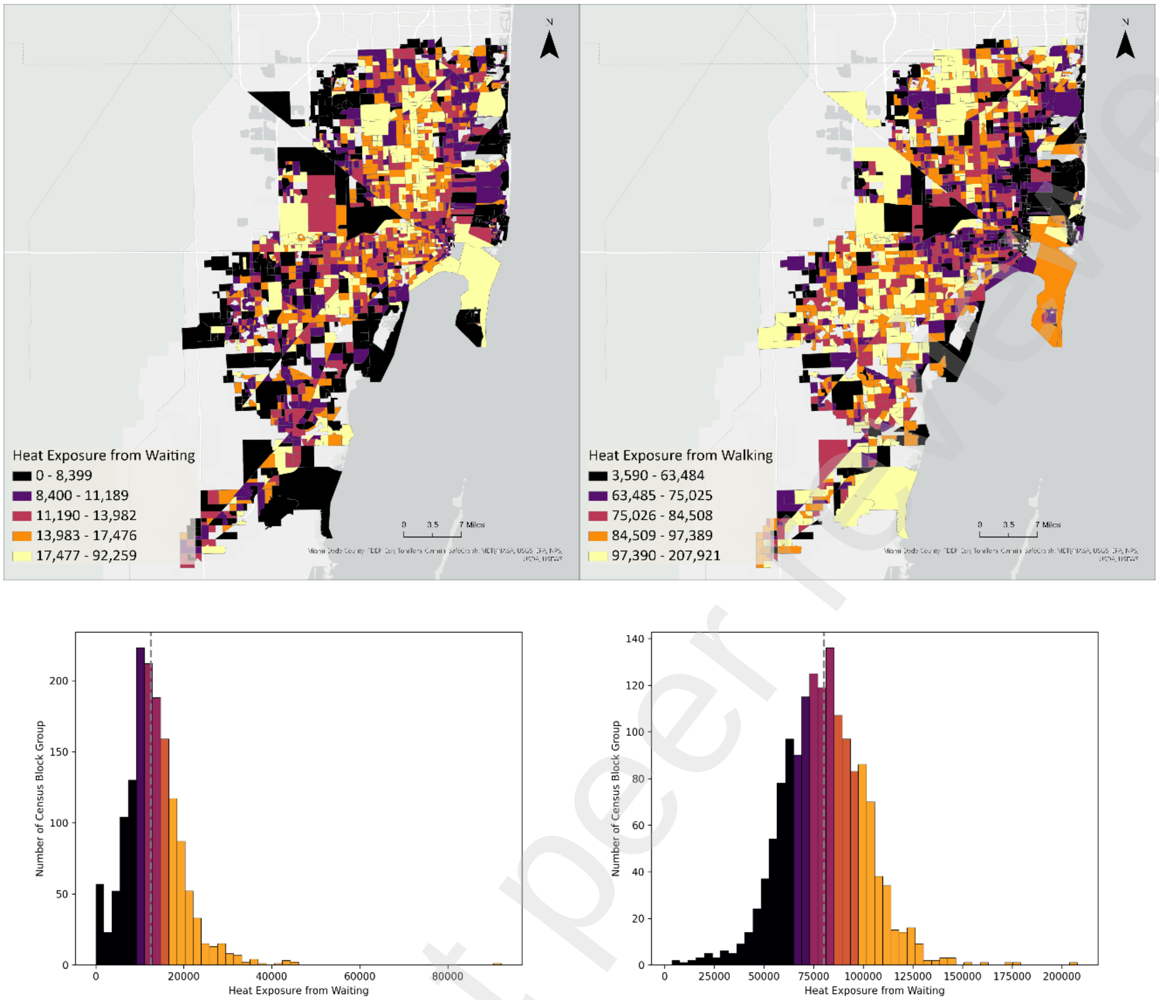

Figure 4: Heat exposure from walking and waiting. Map symbols are generated with quantile classification.

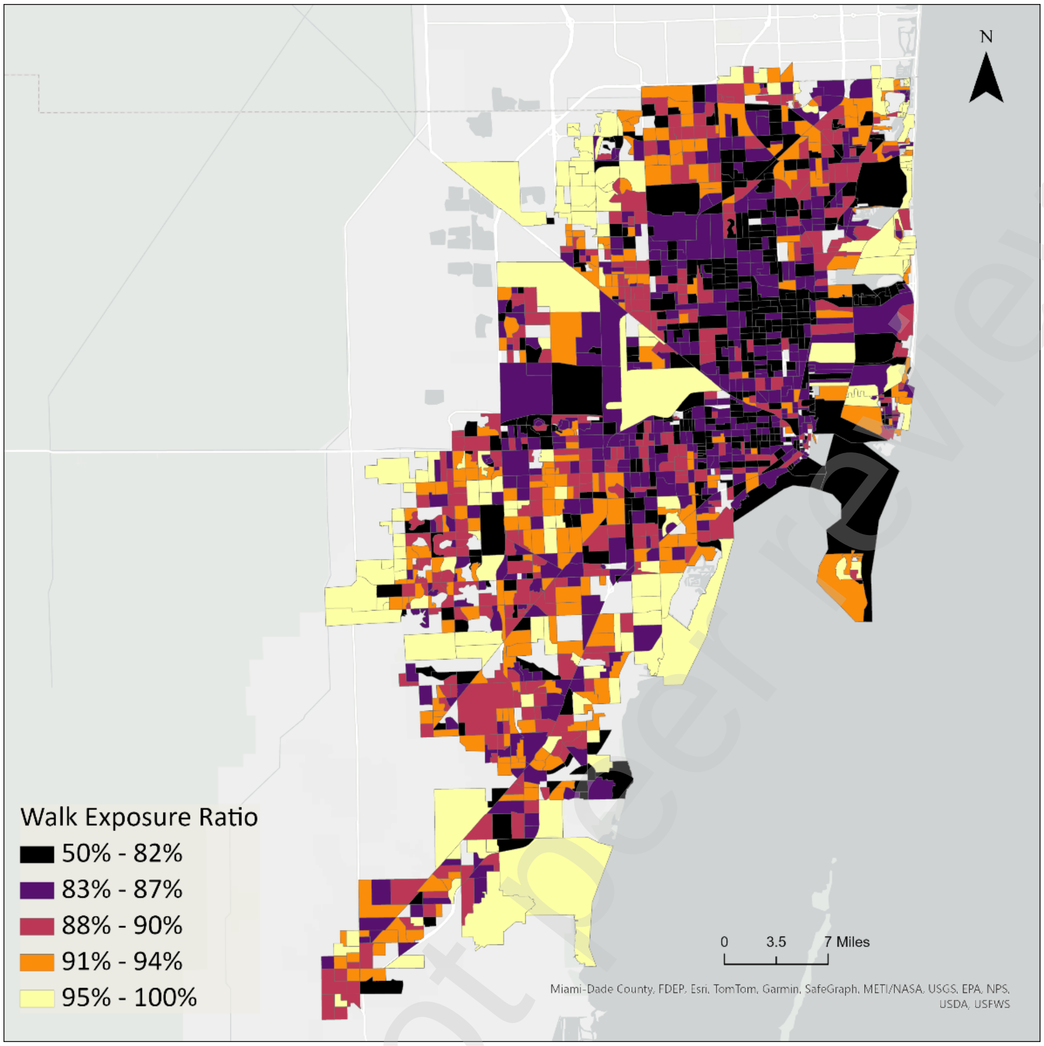

Figure 5: Proportion of exposure due to walking. Maps are generated with quantile classification.

Figure 6 visualizes the heat contribution of each street link and bus stop. We find that only very small number of street links contributes to the total heat exposure. Out of 1,066,000 street links, only 98,879 street links generate heat exposure. Meanwhile, the distribution of heat contribution is highly uneven. The top 5,000 street segments generating heat exposure, which is 5% of street links with nonzero heat generation and less than 0.5%

of all street links, account for 60% of the heat exposure generation on roads. This means that authorities could concentrate intervention efforts on a small number of road links in the sidewalk network, such as adding tree canopies and add sidewalk shelters, to reduce the heat exposure of the majority of the transit riders. As an example, the mere top 100 street segments, whose length is only 16km meters in total, account for almost 10% of the heat exposure. This finding provides actionable information for the authorities to address the heat issue in a very practical, efficient, and cost-effective manner.

Meanwhile, the heat exposure at bus stops is not negligible. Among the 8,164 bus stops, only at 3,987 bus stops (less than half) are riders exposed to heat, and the top 400 bus stops (top 5%) account for 67% of the total heat exposure at bus stops. This resonates well with and complements our findings above that targeted interventions could substantially reduce the heat exposure of transit passengers at very low costs. In fact, due to the nature of bus stops, it is much easier to install shelter than the sidewalk in both human labor and economic senses, and the installation of bus shelters is also positively associated with other factors such as ridership, safety, and revenue (Ewing, 2000; Kim et al., 2020).

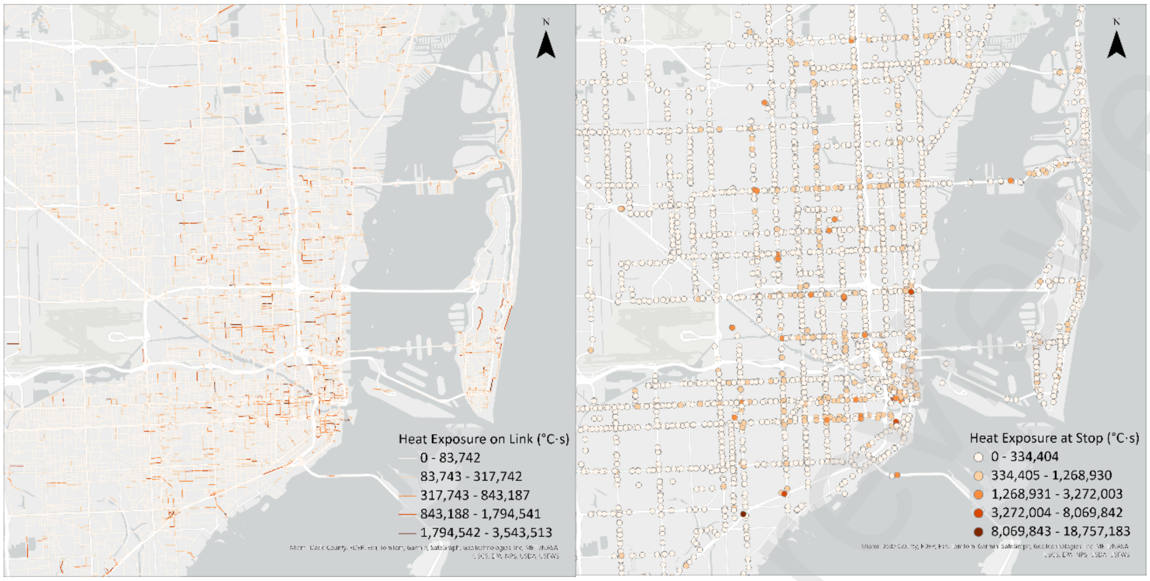

Figure 6: Heat exposure on road links and bus stops. Maps are generated with natural break Jenks classification.

Figure 7 further combine the two sources of heat together and aggregate them to each census block group. As a star-shape public transit system, which heavily depends on transfers near the downtown, it is intuitive and natural to observe that most of the generated heat are from the heart of the city. Meanwhile, it is also interesting that the high-heat-contribution areas can also have much lower heat intensity for local residents (origin-based) and lower heat intensity for other traveler to there (destination-based), which means the areas that contribute the most to the heat can have a much lower experienced heat exposure for local residents. This also resonates well with the discrepancy between MRT and THEI measures.

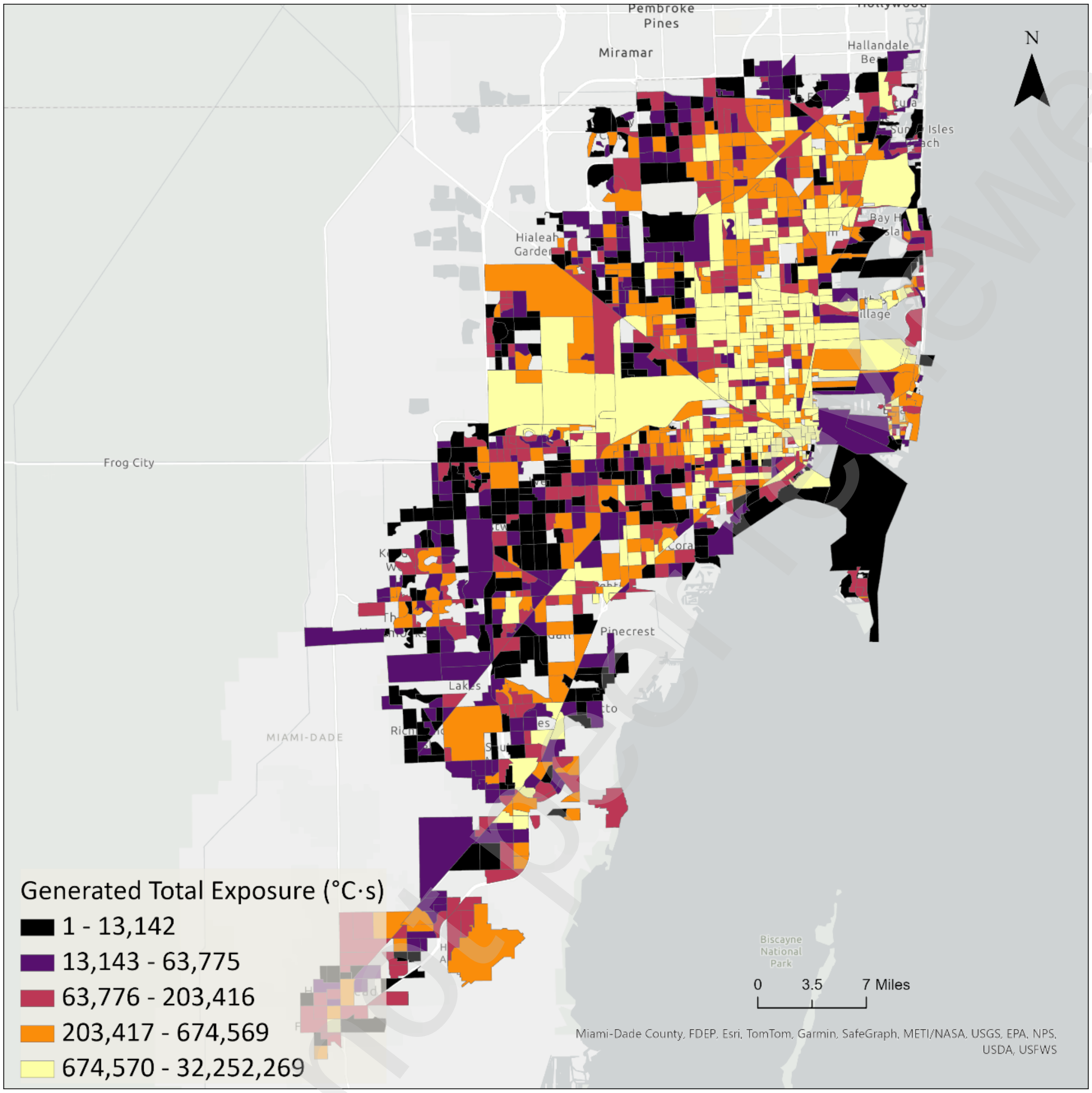

Figure 7: Generated total exposure for each census block groups. Symbols are generated with quantile classification.

5. Discussion and Conclusion

Our spatiotemporal analyses in Miami offer multiple practical insights for future research and planning works.

First, despite the urban heat island effect, the transit heat exposure for city residents may not necessarily be higher. In fact, with high-frequency transit service, connected walking infrastructure, and well-optimized timetable, Miami downtown has much lower exposure intensity than other suburbs and nearby urban outskirt, despite having similar or even higher local feels-like temperature.

Second, there is a discrepancy between mean THEI, which can be considered as a *behavior-based* heat exposure, and localized heat exposure (MRT), which is a *place-based* heat exposure, as shown in Figure 8. It is noteworthy that the two measures follow different distribution across space: the areas with extensive public transit and sidewalk infrastructure like the downtown core, despite having higher local heat exposure, can have relatively lower perceived heat exposure via mobility. On the other hand, the areas with lower local heat exposure can also have very high heat exposure by transportation. It is important to point out that although localized exposure is also useful in other contexts, it does not accurately represent the heat experience of the public transit users, who spent most of their time indoors (Kuras et al., 2017) and suffer most of their heat exposure outside the origin. In that sense, THEI is a more accurate and nuanced proximation to public transit users' experience, as traditional place-based metrics may not capture the full spectrum of heat exposure people face in the public transit contexts.

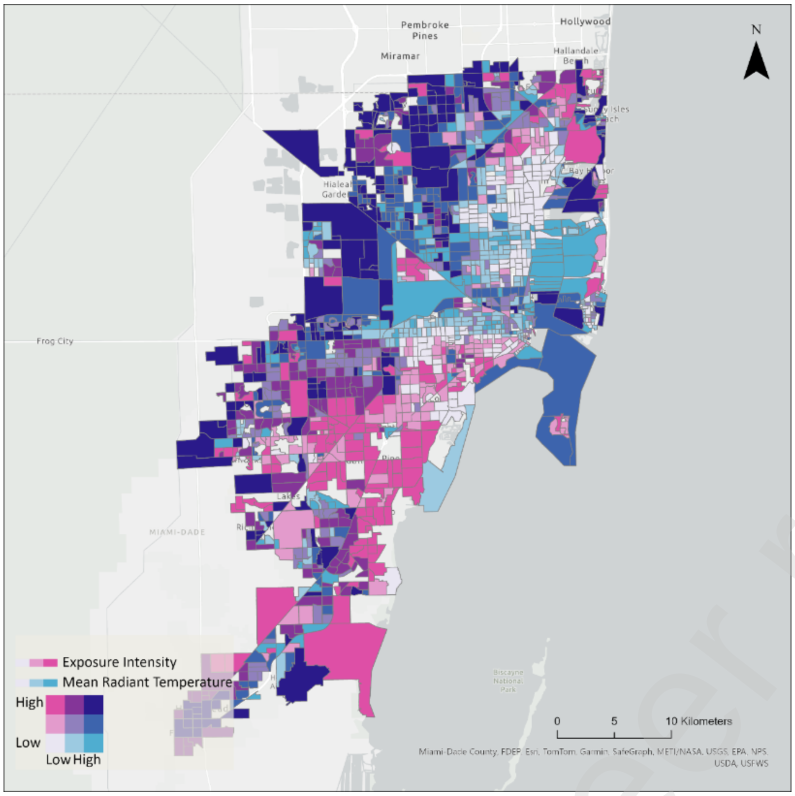

Figure 8: Bivariate map of Miami's mean THEI (mobility-based heat exposure) and mean radiant temperature (local heat exposure). Map symbols are generated with 3*3 quantile classification.

Third, this paper shows that between walking and waiting, walking is the primary source of transit heat exposure in Miami-Dade County. This finding suggests local governments should prioritize reducing walking exposure during future intervention. Possible actions include the optimization of bus timetable to minimize the walking time and creating more shades, primarily tree canopies, on critical street links as we show in the network-based analysis.

Fourth, our analyses show that a very small percentage of road links and bus stops contribute to the majority of heat exposure for all public transit users. This finding points out a practical and efficient solution to the heat exposure problem: it is possible to address a few critical street links and bus stops with accurate, targeted interventions to reduce heat exposure for a large number of people across a broad area.

Finally, although heat exposure during waiting times at bus stops are not the dominating factor, fixing this issue could be a much easier and more effective intervention. For example, some recent thermal technological progress, such as natural cooling stations, can be enacted at bus stops but not on road links. This can decrease the feels-like temperature at the stops to a lower level than on the roads, providing more potentials for heat reduction. Meanwhile, as road works and improvement are usually out of the jurisdiction of public transit authorities, the intervention on the bus stop level is also more practical in the politics and legal sense.

There are multiple topics that future studies can further address. First, although traditional *place-centric* measures, i.e., measuring the heat experience of users by their home/local temperature, have been extensively proven to be useful, our analyses pointed out the urgent need to adopt a *behavior-centric* or *mobility-centric approach* to measure people's heat exposure experience. In other sense, local place-based measures are not an accurate representation of people's heat experience. Note that this insight applies to all people, although it may be more pronounced among public transit riders. For example, a drivers' perceived heat exposure would not be their local heat situation around their home, but rather more about the heat near their destination or parking. To achieve this goal, we need a coordinated endeavor to integrate the existing research on both heat exposure research and travel behavior research. Second, with the THEI system we introduce above, future research can use the measure to optimize exposure in a city or for a public transit system. While it is hard to control the temperature, it is within the power of transit planners and transit authorities to conduct system redesign to reduce exposure time. Future research could also explore strategies for positioning tree canopies or bus stops to help lower temperatures.

Future studies could also try to incorporate other factors that can contribute to heat exposure in transit trips, such as how thermal comfort might be affected by vehicle crowding and terrain elevation. Finally, the method employed in this study first determines the fastest trip itinerary between a given OD pair and subsequently calculates heat exposure. Future research could try to incorporate the heat exposure during walking along street links into the routing algorithm to reflect how some pedestrians choose their trip itineraries trying to travel time and heat exposure costs.

Reference

Arbex, R., & Cunha, C. B. (2020). Estimating the influence of crowding and travel time variability on accessibility to jobs in a large public transport network using smart card big data. *Journal of Transport Geography*, *85*, 102671.

Benmarhnia, T., Deguen, S., Kaufman, J. S., & Smargiassi, A. (2015). Vulnerability to heat-related mortality: A systematic review, meta-analysis, and meta-regression analysis. *Epidemiology*, *26*(6), 781–793.

Błażejczyk, K., Jendritzky, G., Bröde, P., Fiala, D., Havenith, G., Epstein, Y., Psikuta, A., & Kampmann, B. (2013). An introduction to the universal thermal climate index (UTCI). *Geographia Polonica*, *86*(1), 5–10.

Bowman, L. A., & Turnquist, M. A. (1981). Service frequency, schedule reliability and passenger wait times at transit stops. *Transportation Research Part A: General*, *15*(6), 465–471. https://doi.org/10.1016/0191-2607(81)90114-X

Cheung, P. K. (2018). Comparing the cooling effects of a tree and a concrete shelter using PET and UTCI. *Building and Environment*, *130*, 49–61.

Crowley, K. (2023, September 13). *Miami playground surface hits 177.9 degrees amid record-breaking heat in Florida*. USA TODAY. https://www.usatoday.com/story/news/weather/2023/08/11/miami-playground-measures-178-degrees-hot-surfaces/70574217007/

Curriero, F. C., Heiner, K. S., Samet, J. M., Zeger, S. L., Strug, L., & Patz, J. A. (2002). Temperature and mortality in 11 cities of the eastern United States. *American Journal of Epidemiology*, *155*(1), 80–87.

Deschenes, O. (2014). Temperature, human health, and adaptation: A review of the empirical literature. *Energy Economics*, *46*, 606–619.

Dong, J., Peng, J., He, X., Corcoran, J., Qiu, S., & Wang, X. (2020). Heatwave-induced human health risk assessment in megacities based on heat stress-social vulnerability-human exposure framework. *Landscape and Urban Planning*, *203*, 103907.

Dzyuban, Y., Hondula, D. M., Coseo, P. J., & Redman, C. L. (2021). Public transit infrastructure and heat perceptions in hot and dry climates. *International Journal of Biometeorology*, 1–12.

Ebi, K. L., Vanos, J., Baldwin, J. W., Bell, J. E., Hondula, D. M., Errett, N. A., Hayes, K., Reid, C. E., Saha, S., & Spector, J. (2021). Extreme weather and climate change: Population health and health system implications. *Annual Review of Public Health*, *42*(1), 293–315.

Ewing, R. (2000). Asking transit users about transit-oriented design. *Transportation Research Record*, *1735*(1), 19–24.

Fraser, A. M., & Chester, M. V. (2017). Transit system design and vulnerability of riders to heat. *Journal of Transport & Health*, *4*, 216–225.

Fraser, A. M., Chester, M. V., Eisenman, D., Hondula, D. M., Pincetl, S. S., English, P., & Bondank, E. (2017). Household accessibility to heat refuges: Residential air conditioning, public cooled space, and walkability. *Environment and Planning B: Urban Analytics and City Science*, *44*(6), 1036–1055.

Google Developers. (2020). *GTFS Static Overview | Static Transit | Google Developers*. https://developers.google.com/transit/gtfs/

Gu, X., Chen, P., & Fan, C. (2024). Socio-demographic inequalities in the impacts of extreme temperatures on population mobility. *Journal of Transport Geography*, *114*, 103755.

Higgins, C. D., Xi, Y. L., Widener, M., Palm, M., Vaughan, J., Miller, E. J., DeJohn, A., & Farber, S. (2022). Calculating place-based transit accessibility. *Journal of Transport and Land Use*, *15*(1), 95–116.

Hsu, A., Sheriff, G., Chakraborty, T., & Manya, D. (2021). Disproportionate exposure to urban heat island intensity across major US cities. *Nature Communications*, *12*(1), 2721.

Huang, X., Jiang, Y., & Mostafavi, A. (2024). The emergence of urban heat traps and human mobility in 20 US cities. *Npj Urban Sustainability*, *4*(1), 6.

Iseki, H., & Tingstrom, M. (2014). A new approach for bikeshed analysis with consideration of topography, street connectivity, and energy consumption. *Computers, Environment and Urban Systems*, *48*, 166–177.

Karner, A. (2018). Assessing public transit service equity using route-level accessibility measures and public data. *Journal of Transport Geography*, *67*, 24–32. https://doi.org/10.1016/J.JTRANGEO.2018.01.005

Karner, A., Hondula, D. M., & Vanos, J. K. (2015). Heat exposure during non-motorized travel: Implications for transportation policy under climate change. *Journal of Transport & Health*, *2*(4), 451–459.

Keellings, D., & Waylen, P. (2014). Increased risk of heat waves in Florida: Characterizing changes in bivariate heat wave risk using extreme value analysis. *Applied Geography*, *46*, 90–97.

Kim, J. Y., Bartholomew, K., & Ewing, R. (2020). Another one rides the bus? The connections between bus stop amenities, bus ridership, and ADA paratransit demand. *Transportation Research Part A: Policy and Practice*, *135*, 280–288.

Klein, T., & Anderegg, W. R. (2021). A vast increase in heat exposure in the 21st century is driven by global warming and urban population growth. *Sustainable Cities and Society*, *73*, 103098.

Kuras, E. R., Hondula, D., & Brown-Saracino, J. (2015). Heterogeneity in individually experienced temperatures (IETs) within an urban neighborhood: Insights from a new approach to measuring heat exposure. *International Journal of Biometeorology*, *59*, 1363–1372.

Kuras, E. R., Richardson, M. B., Calkins, M. M., Ebi, K. L., Hess, J. J., Kintziger, K. W., Jagger, M. A., Middel, A., Scott, A. A., & Spector, J. T. (2017). Opportunities and challenges for personal heat exposure research. *Environmental Health Perspectives*, *125*(8), 085001.

Lanza, K., & Durand, C. P. (2021). Heat-moderating effects of bus stop shelters and tree shade on public transport ridership. *International Journal of Environmental Research and Public Health*, *18*(2), 463.

Li, R., Chester, M. V., Hondula, D. M., Middel, A., Vanos, J. K., & Watkins, L. (2023). Repurposing mesoscale traffic models for insights into traveler heat exposure. *Transportation Research Part D: Transport and Environment*, *114*, 103548.

Li, X. (2021). Investigating the spatial distribution of resident's outdoor heat exposure across neighborhoods of Philadelphia, Pennsylvania using urban microclimate modeling. *Sustainable Cities and Society*, *72*, 103066.

Li, X., & Wang, G. (2021). GPU parallel computing for mapping urban outdoor heat exposure. *Theoretical and Applied Climatology*, *145*(3–4), 1101–1111. https://doi.org/10.1007/s00704-021-03692-z

Liu, L., Kar, A., Tokey, A. I., Le, H. T., & Miller, H. J. (2023). Disparities in public transit accessibility and usage by people with mobility disabilities: An evaluation using high-resolution transit data. *Journal of Transport Geography*, *109*, 103589.

Liu, L., & Miller, H. J. (2020). Measuring risk of missing transfers in public transit systems using high-resolution schedule and real-time bus location data. *Urban Studies*, *58*(15), 3140–3156.

Liu, L., Porr, A., & Miller, H. J. (2022). Realizable accessibility: Evaluating the reliability of public transit accessibility using high-resolution real-time data. *Journal of Geographical Systems*, 1–23.

Mayer, H., & Höppe, P. (1987). Thermal comfort of man in different urban environments. *Theoretical and Applied Climatology*, *38*(1), 43–49. https://doi.org/10.1007/BF00866252

McAllister, C., Stephens, A., & Milrad, S. M. (2022). The heat is on: Observations and trends of heat stress metrics during Florida summers. *Journal of Applied Meteorology and Climatology*, *61*(3), 277–296.

McMichael, C. (2020). Human mobility, climate change, and health: Unpacking the connections. *The Lancet Planetary Health*, *4*(6), e217–e218.

Miao, Q., Welch, E. W., & Sriraj, P. (2019). Extreme weather, public transport ridership and moderating effect of bus stop shelters. *Journal of Transport Geography*, *74*, 125–133.

Microsoft. (2024). *GitHub—Microsoft/USBuildingFootprints* [Computer software]. Microsoft. https://github.com/microsoft/USBuildingFootprints (Original work published 2018)

National Agriculture Imagery Program. (2023). *National Agriculture Imagery Program—NAIP Hub Site*. https://naip-usdaonline.hub.arcgis.com/

Nazarian, N., & Lee, J. K. (2021). Personal assessment of urban heat exposure: A systematic review. *Environmental Research Letters*, *16*(3), 033005.

NREL. (2024). *NSRDB: National Solar Radiation Database*. https://nsrdb.nrel.gov/

Obiakor, M., Ezeonyejiaku, C., & Mogbo, T. (2012). Effects of vegetated and synthetic (impervious) surfaces on the microclimate of urban area. *Journal of Applied Sciences and Environmental Management*, *16*(1), 85–94.

OpenMobilityData. (2023). *OpenMobilityData—Public transit feeds from around the world*. https://transitfeeds.com/

Pereira, R. H. M., Saraiva, M., Herszenhut, D., Braga, C. K. V., & Conway, M. W. (2021). r5r: Rapid realistic routing on multimodal transport networks with r 5 in r. *Findings*, 21262.

Sami, I., & Keith, L. (2023). How do streetcar transit users and streetcar decision-makers perceive heat risk? *Journal of Public Transportation*, *25*, 100045.

Shandas, V., Voelkel, J., Williams, J., & Hoffman, J. (2019). Integrating satellite and ground measurements for predicting locations of extreme urban heat. *Climate*, *7*(1), 5.

Stewart, A. F., & Byrd, A. M. (2023). Half-(head)way there: Comparing two methods to account for public transport waiting time in accessibility indicators. *Environment and Planning B: Urban Analytics and City Science*, *50*(8), 2187–2202. https://doi.org/10.1177/23998083221137077

Thorsson, S., Rocklöv, J., Konarska, J., Lindberg, F., Holmer, B., Dousset, B., & Rayner, D. (2014). Mean radiant temperature–A predictor of heat related mortality. *Urban Climate*, *10*, 332–345.

Turek-Hankins, L. L., Hino, M., & Mach, K. J. (2020). Risk screening methods for extreme heat: Implications for equity-oriented adaptation. *Plos One*, *15*(11), e0240841.

US Census Bureau. (2020). *2016-2020 American community Survey 5-year estimates*. https://data.census.gov/table

U.S Geological Survey. (2023). *Lidar Point Cloud—USGS National Map 3DEP Downloadable Data Collection | USGS Science Data Catalog*. https://data.usgs.gov/datacatalog/data/USGS:b7e353d2-325f-4fc6-8d95-01254705638a

Wang, J., & Cao, X. (2017). Exploring built environment correlates of walking distance of transit egress in the Twin Cities. *Journal of Transport Geography*, *64*, 132–138.

Wong, K. V., Paddon, A., & Jimenez, A. (2013). Review of world urban heat islands: Many linked to increased mortality. *Journal of Energy Resources Technology*, *135*(2), 022101.

World Weather Online. (2024). *World Weather Online*. WorldWeatherOnline.Com. https://www.worldweatheronline.com/

Yau, Y., & Chew, B. (2014). A review on predicted mean vote and adaptive thermal comfort models. *Building Services Engineering Research and Technology*, *35*(1), 23–35.

Yin, Z., Liu, Z., Liu, X., Zheng, W., & Yin, L. (2023). Urban heat islands and their effects on thermal comfort in the US: New York and New Jersey. *Ecological Indicators*, *154*, 110765.